Int. J. Multiphase Flow Vol. 18, No. 2, pp. 181–194, 1992
Printed in Great Britain.

0301-9322/92 $5.00 + 0.00

EXPERIMENTS ON PARTICLE DISPERSION IN A TURBULENT MIXING LAYER

K. HISHIDA, A. ANDO and M. MAEDA
Department of Mechanical Engineering, Keio University, 3-14-1 Hiyoshi, Kohoku-ku, Yokohama 223, Japan

(Received 8 June 1990; in revised form 9 August 1991)

Abstract—The dispersion of solid particles in a turbulent shear layer has been investigated experimentally to clarify the dominant factors which govern the particle motion in turbulent gas flow. Spherical glass particles were loaded at the origin of a two-dimensional mixing layer. Flow measurements were carried out by a modified laser Doppler anemometer which enabled the measurement of both particle and gas phase velocities and particle number density. The particle disperison strongly depended on the ability of the particles to follow the motion of large-scale eddies and was well-classified by the Stokes number (St). The range of St values covered in the present study turned out to involve three different stages of particle dispersion. It was confirmed from the experiments (with $0.5 < St < 2.5$) that the particle dispersion coefficients became larger than the eddy diffusivity of the gas phase, i.e. the particles in the developing shear layer dispersed more than the fluid phase.

Key Words: two-phase turbulence, gas–solid flow, particle diffusion, shear flow, LDV

1. INTRODUCTION

The analysis of turbulent flows containing small droplets or particles is required in many significant industrial processes. Fluid mechanics in such two-phase flows remain somewhat unexplored due to the very complex interaction between the dispersed and continuous phase. Therefore, a clarification of the complicated turbulent motions of the dispersed and continuous phases could contribute to an analysis of the heat and mass transfer processes in practical two-phase flow systems for a further improvement of equipment.

Turbulent characteristics in two-phase flows have been measured rarely in the last decade because of the lack of effective measuring techniques. Recently, some investigators have tried to obtain direct information regarding the velocities of both phases using laser Doppler velocimetry (Lee & Durst 1982; Hishida *et al.* 1984; Modaress *et al.* 1984; Shuen *et al.* 1985; Parthasarathy & Faeth 1987). These studies have succeeded in obtaining local information on not only the mean velocities but also turbulent properties and particle concentration. The present authors' group has investigated the particle motion and turbulent gas flows to correlate the local characteristics of turbulence and heat transfer. A series of investigations in connection with turbulent dispersed two-phase flows has been reported for backward step flow (Maeda *et al.* 1982), wall jets (Hishida *et al.* 1986), free jets (Fleckhaus *et al.* 1987) and confined jets (Hishida *et al.* 1987, 1989a, b). These results indicated a modification of gas phase turbulence due to the presence of particles.

Considerable efforts regarding numerical predictions have also been made, where the methods may be divided in two main categories, namely the Eulerian approach and the Lagrangian approach. In the Eulerian approach the dispersed phase is treated as a continuum, and has been reported by several researchers (Danon *et al.* 1977; Melville & Bray 1979; Elgobashi *et al.* 1984; Chen & Wood 1986; Picart *et al.* 1986; Lee & Chung 1987). The Lagrangian approach predicts the particle motion in the continuous phase by solving the equation of particle motion directly (Shuen *et al.* 1985; Parthasarathy & Faeth 1987; Milojevic & Durst 1989; Berlemont *et al.* 1990). However, despite some successes, difficulties still remain in connection with models representing the various physical aspects of turbulent particle motion. Consequently, it becomes imperative to conduct an experiment to yield data which improve the basic understanding of the fundamental phenomena.

It is from this point of view that the present experimental study has been carried out on the particle motion in a plane mixing layer, in order to clarify the particle dispersion in a simple turbulent shear flow whose turbulent motion directly affects the particle trajectories.

Generally, particle motion in turbulent flow depends mainly on the ratio of the time scale of particle-inertia to that of turbulence. However, it remains unexplored as to which turbulence time scale is the appropriate scaling parameter for particle-inertia. Snyder & Lumley (1971), Calabrese & Middleman (1979) and Wells & Stock (1983) studied the particle dispersion in a steady isotropic grid turbulence and the turbulence in the central region of fully-developed pipe flow. There was no agreement on the relevant time scales in these studies, since both the micro and the integral time scales were used.

The plane mixing layer in single-phase flow, which is one of the simplest free shear layers, has been well studied by numerous investigators (e.g. Brown & Roshko 1974; Winant & Browand 1974; Hussain & Zaman 1985) and some features regarding the relation between the development and large-scale structures of the shear layer have been identified.

Chein & Chung (1987, 1988) and Tang *et al.* (1989) reported the numerical calculation concerning particle dispersion in a shear layer. They pointed out that flow behaviors were simulated by taking account of large-scale eddies in the turbulent flow, and confirmed that particles could mix faster than the fluid over a certain range of Stokes number. However, there is little experimental data on the effect of large-scale eddies on the particle dispersion. Also, detailed information on local particle velocities, such as mean velocity, velocity fluctuations and their correlation, are required for evaluating the numerical prediction of particle motion. Therefore, the objective of the present study is to obtain experimental data on both particle velocity and particle dispersion in a two-dimensional mixing layer, where some characteristics of large-scale turbulence have been well-examined in previous studies. Detailed measurements of particle and gas velocities and particle number densities are presented using a modified laser Doppler anemometer with particle size discrimination.

2. EXPERIMENTAL SET UP AND FLOW CONDITIONS

The experimental flow configuration is shown in figure 1, together with Cartesian coordinates with the origin located at the center of the trailing edge. The streamwise direction was the X-axis and the direction perpendicular to the splitter plate was the Y-axis. A suction-type wind tunnel was installed vertically, as shown in figure 2, for the convenience of particle loading. Air was passed through a mixing chamber where aluminum powder of approx. 1 μm was added by the tracer feeder. Then, the flow was divided into two streams and passed through the settling duct, which contained screens to damp large-scale turbulence, and through a 7:1 contraction to the test section which was 150 × 100 mm in cross-section and 450 mm long. The chamber and contraction were divided in half by the splitter plate which was made of thin aluminum plates which were tapered uniformly through the duct. The end of the splitter plate was made of two 50 mm long and 0.3 mm thick aluminum plates with a constant spacing of 0.57 mm to minimize the effect of the resulting wakes on the initial mixing region. Glass particles were added to the mixing layer from the opening of the splitter plate and separated downstream of the test section from the gas phase by a cyclone.

In the present study, the gas phase velocities, U_1 and U_2, were set at 13 and 4 m/s, respectively. Turbulence intensities in the streamwise direction were about 0.9% for the higher velocity and about 2% for the lower velocity flow.

Three kinds of glass particles with a mean diameter of d_p of 42, 72 and 135 μm were added to the mixing layer. The mass flow rates for each particle were 7.5 and 20.9 and 20.43 g/s, respectively. Figure 3 indicates particle size distributions. The mean diameter, the standard deviation in diameter σ and the particle Stokesian relaxation time τ_p for each particle are also tabulated.

A three-beam laser Doppler velocimeter was used for simultaneous two-component velocity measurements of the particle and gas phase, which permitted particle size discrimination using the light scattering intensity method (Fleckhaus *et al.* 1987).

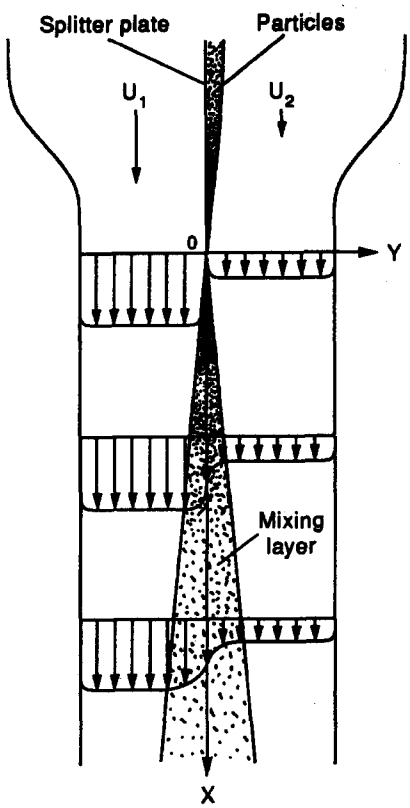

Figure 1. Flow configuration

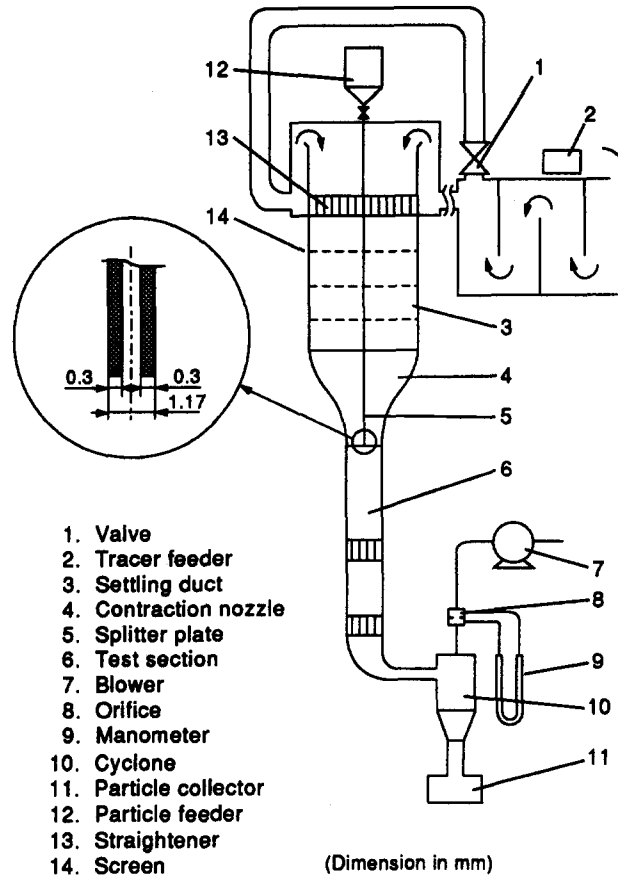

Figure 2. Experimental wind tunnel.

Diameter d_p [μm]	Standard deviation σ [μm]	Density ρ [kg/m^3]	Relaxation time [s]
42	5.4	2590	0.014
72	7.5		0.041
135	7.9		0.144

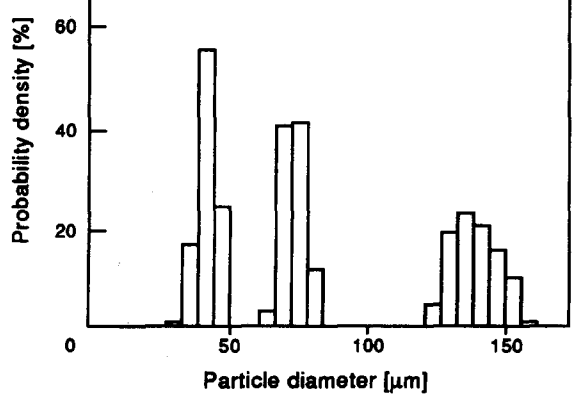

Figure 3. Particle size distribution.

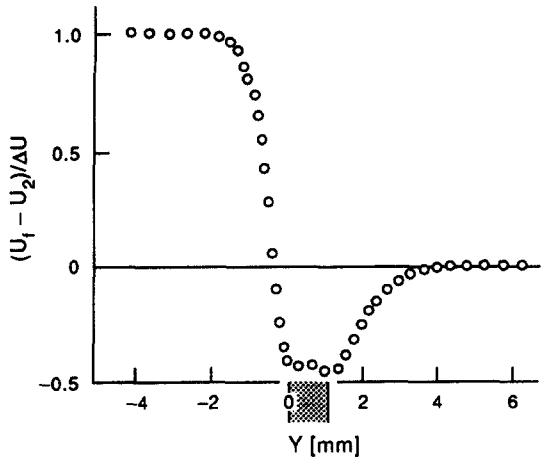

Figure 4. Initial condition of mean gas velocity.

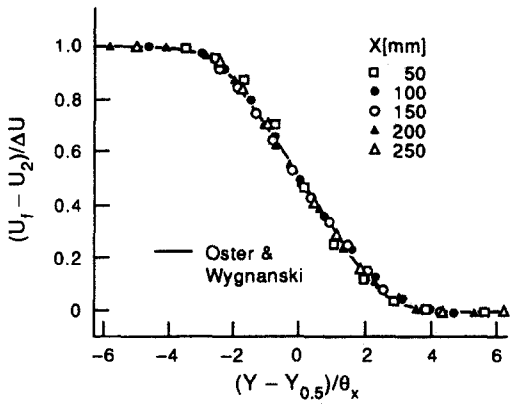

Figure 5. Mean velocity distributions (single phase).

3. RESULTS AND DISCUSSION

3.1. Single-phase Flow

Figure 4 shows the inlet condition of the streamwise mean velocity at $X = 0.5$ mm. Generally, the boundary layer which develops over the splitter plate strongly affects the development of the mixing layer. The velocity profiles indicated in figure 4 confirm a good fit to the exact solution of the laminar boundary layer for both higher and lower velocity flows. The Reynolds number based on the momentum thickness of the boundary layer on the higher velocity side θ_c, and U_1 was approx. 200.

The distribution of the mean velocity and the RMS of the velocity fluctuation in the streamwise direction u' are shown in figures 5 and 6, respectively, where $Y_{0.5}$ means the location at half of ΔU. The solid line in figures 5 and 6 is the fully-developed two-dimensional mixing layer experiment reported by Oster & Wygnanski (1982). In the present flow, the effect of the splitter plate is barely noticeable for locations over $X = 100$ mm. The profiles of mean velocity are in good agreement with the result of Oster & Wygnanski (1982). The maximum values of turbulence intensity decrease with the downstream distance and decay below the values of Oster & Wygnanski (1982).

The flow visualization by Brown & Roshko (1974) showed that coherent structures exist in the turbulent shear flows and the velocity fluctuation at the edge of the shear layer exhibited periodicity due to the passage of large-scale eddies. In the present experiment, the time series of instantaneous velocity was measured by a hot-wire anemometer in a single-phase flow for the

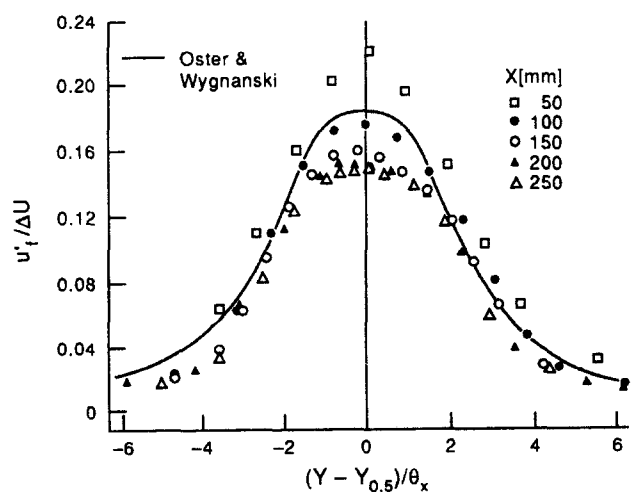

Figure 6. Velocity fluctuation distributions (single phase).

evaluation of turbulence scales. Figure 7 shows an example of a frequency analysis of the streamwise velocity fluctuation at $X = 200$ mm at the outer edge of the higher velocity stream ($Y = -12$ mm). Hussain & Zaman (1985) estimated the local Strouhal number, Sr, based on the momentum thickness of the mixing layer, θ_x, and the most probable frequency of the main stream velocity fluctuation, f_m, and found that it has a constant value for both the initial mixing region and the self-preserving region. In the present study, θ_x and Sr are defined by

$$\theta_x = \int_{-\infty}^{+\infty} \frac{U - U_2}{\Delta U}\left(1 - \frac{U - U_2}{\Delta U}\right) dy \qquad [1]$$

and

$$\mathrm{Sr} = \frac{f_m \cdot \theta_x}{U_m}, \qquad [2]$$

respectively; $U_m = (U_1 + U_2)/2$ and U is the streamwise time-averaged velocity.

Figure 8 shows the evaluated local Sr value and local momentum thickness. The Sr value approaches a constant value of 0.55 after $X = 100$ mm, but $\mathrm{Sr} < 0.55$ upstream of $X = 100$ mm. The effect of the splitter plate on the construction of large-scale eddy motion could be negligible for locations beyond $X = 100$ mm.

Uncertainties in the measurement of the mean velocity and fluctuation are estimated at the 95% confidence interval; for the normalized mean velocity $(U - U_2)/\Delta U$ the uncertainty was ± 0.046 at $Y = 150$ mm and $X = 0$ mm, and ± 0.035 at $X = 250$ mm and $Y = 0$ mm; for the velocity fluctuation, $u'/\Delta U$, the uncertainty was ± 0.080 at $X = 150$ mm and $Y = 0$ mm, and ± 0.072 at $X = 250$ mm and $Y = 0$ mm.

3.2. Two-phase Flow

3.2.1. Characteristic time scales of particles and large eddies

The ability of a particle to follow the turbulent motion of its surrounding flow strongly depends on the ratio of the particle relaxation time to the characteristic time scale of the flow field. Since the present study intends to clarify the effect of coherent structure on the particle motion, the characteristic time scale of a large-scale eddy is estimated by the following definition of Chein & Chung (1987):

$$\tau_f = \frac{\lambda}{\frac{\Delta U}{2}}, \qquad [3]$$

where λ is the streamwise width of the coherent structure. In the present study λ is obtained from the most probable frequency, f_m, by multiplying it by the convection velocity for the large-scale structure, which is approximated by $(U_1 + U_2)/2$ for a shear layer (Dimotakis & Brown 1976):

$$\lambda = \frac{1}{f_m}\frac{U_1 + U_2}{2}. \qquad [4]$$

The time scales of the large eddies in the present flow condition are indicated in figure 9 by the ○ symbols. The dotted horizontal lines in figure 9 are the particles' Stokesian relaxation times ($\epsilon_p = \rho d_p^2/18\mu$) for the three particle sizes examined in the study. Chein & Chung (1987) studied the effect of τ_f on the particle dispersion by means of a numerical computation. They showed that particles with an intermediate Stokes number ($=\tau_p/\tau_f$) ($0.5 < \mathrm{St} < 5$) might be dispersed further than the fluid and might actually be flung out of the vortex structure. For comparison of Chein & Chung's numerical calculation with the present experimental condition, the ranges of τ_p for the intermediate St values ($0.5 < \mathrm{St} < 5$) are shown by vertical solid lines in figure 9.

3.2.2. Distributions of particle number density

The distributions of particle number density are presented in figures 10(a), (b) and (c) for 135, 72 and 42 μm particles, respectively. The particle number density was measured by counting the

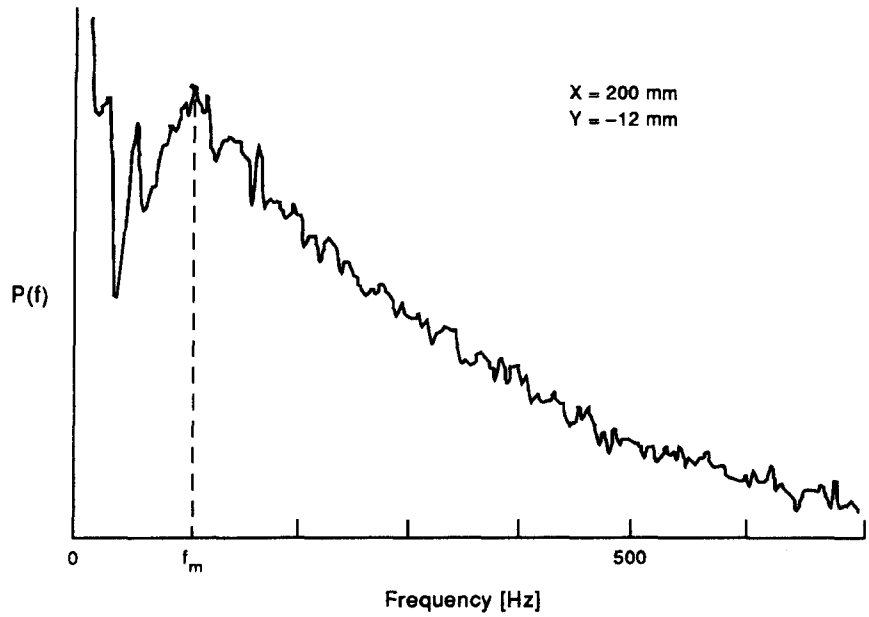

Figure 7. Frequency spectrum of the streamwise velocity on the high-speed side edge of the shear layer.

number of Doppler burst signals of a particle passing through the measuring volume of the LDA in a specific time interval. The vertical scale of these figures is normalized by the maximum value at $X = 100$ mm.

For particles of 135 and 72 μm, the distributions of number density maintain a sharp profile up to $X = 100$ mm. For locations further downstream, the particles disperse in the Y direction and peak values are located around $Y = 0$ mm. Particle dispersion to the low-speed side becomes larger for 72 μm particles as compared with 135 μm particles at $X = 200$ mm downstream of the splitter plate.

In contrast, the 42 μm particles migrate toward the low-speed side of the flow and the peak value of the particle number density shifts to the low-speed side in the streamwise direction and the skewness of the number density distribution becomes large with increasing X.

The phenomena of dispersion toward the low-speed side can be explained as follows. Since the mixing layer spreads out more toward the low-speed side because of the entrainment from the high-speed side, the centerline of the mixing layer shifts to the low-speed side with increasing streamwise distance. Particles, added at the origin of the mixing layer, go straight for a certain distance due to their inertia. Thereafter, particles encounter the vortex structure in the high-speed region with a higher probability. Consequently, particles are strongly affected by the fluid motion from the high-speed toward the low-speed side, and more disperse to the low-speed side.

3.2.3. Distributions of particle mean velocity

The particle streamwise mean velocity is given in figure 11. The distributions upstream of $X = 100$ mm are not discussed because the turbulent structure is considered to be unestablished there. The effect of particle presence on the gas phase flow was examined using a modified LDA with particle size discrimination at several streamwise locations. In the present experimental conditions, the maximum deviation of gas velocity profiles in two-phase flow with respect to velocity profiles in single-phase flow was $< 3\%$ due to the low concentration of particles. Therefore, for comparison the single-phase flow quantities are conjugated in figures 11–14 by solid lines in terms of $(U_f - U_2)/\Delta U$, $u_f'/\Delta U$, $v_f'/\Delta U$ and $\overline{u_f' v_f'}/\Delta U^2$, respectively.

The particle velocities at the exit of the splitter plate are almost the same for the three kinds of particles, approx. 0.9 m/s. Therefore, the mean velocity at $X = 100$ mm corresponds to the ability of the particles to be accelerated. The particle with the smallest relaxation time has a higher velocity at $X = 100$ mm. Further downstream, the 42 μm particles approach the velocity of the gas phase. The velocities of the 72 μm particles at locations of $X = 200$ and 250 mm are higher than that of the 42 μm particles on the low-speed side. The free fall velocities are 0.4 m/s for

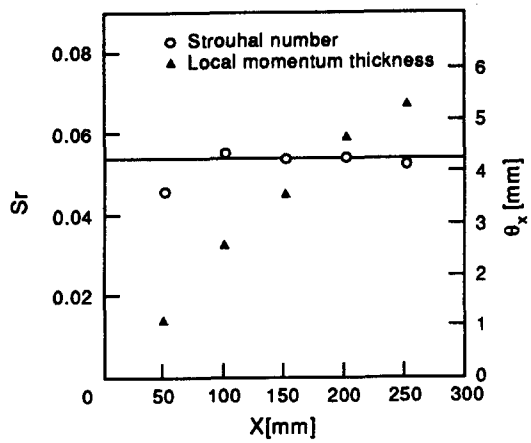

Figure 8. Variation of Sr and the local momentum thickness with downstream distance.

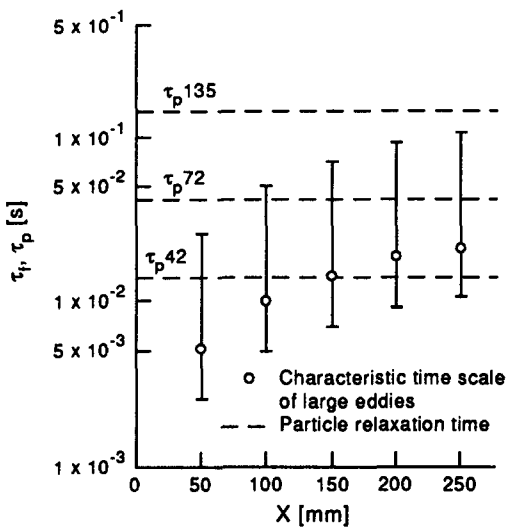

Figure 9. Streamwise variation of the characteristic time of large-scale structure, τ_f.

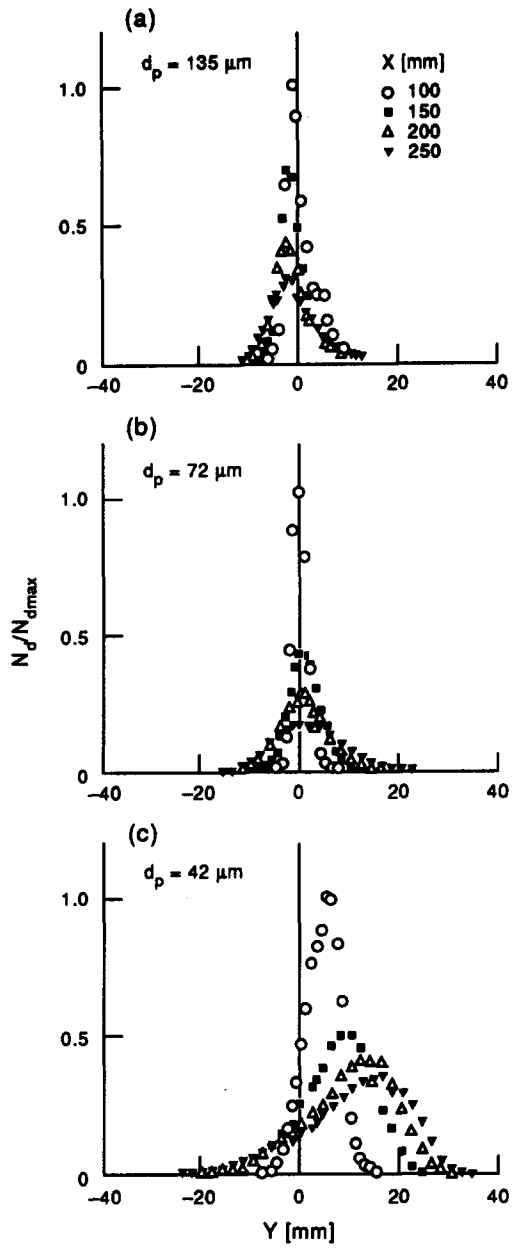

Figure 10. Distributions of particle number density.

the 72 μm particles and 0.14 m/s for the 42 μm particles. The velocity of the 72 μm particles on the low-speed side is somewhat large compared to the free fall velocity. This behavior could be caused by the motion whereby particles on the high-speed side disperse to the low-speed side by catching up the vortex structure and might be flung out of the vortex with higher velocity due to their inertia.

In contrast, the 135 μm particles, whose relaxation time is about 10 times larger than that of 42 μm particles, keep their velocity below that of the gas phase. This size of particles was unable to follow even the mean flow of gas phase motion.

3.2.4. Distributions of particle velocity fluctuation and $\overline{u'v'}$-correlation

The distributions of particle velocity fluctuation in the streamwise and lateral direction are shown in figures 12 and 13, where u' and v' are the RMS (root mean square) values of the velocity fluctuation.

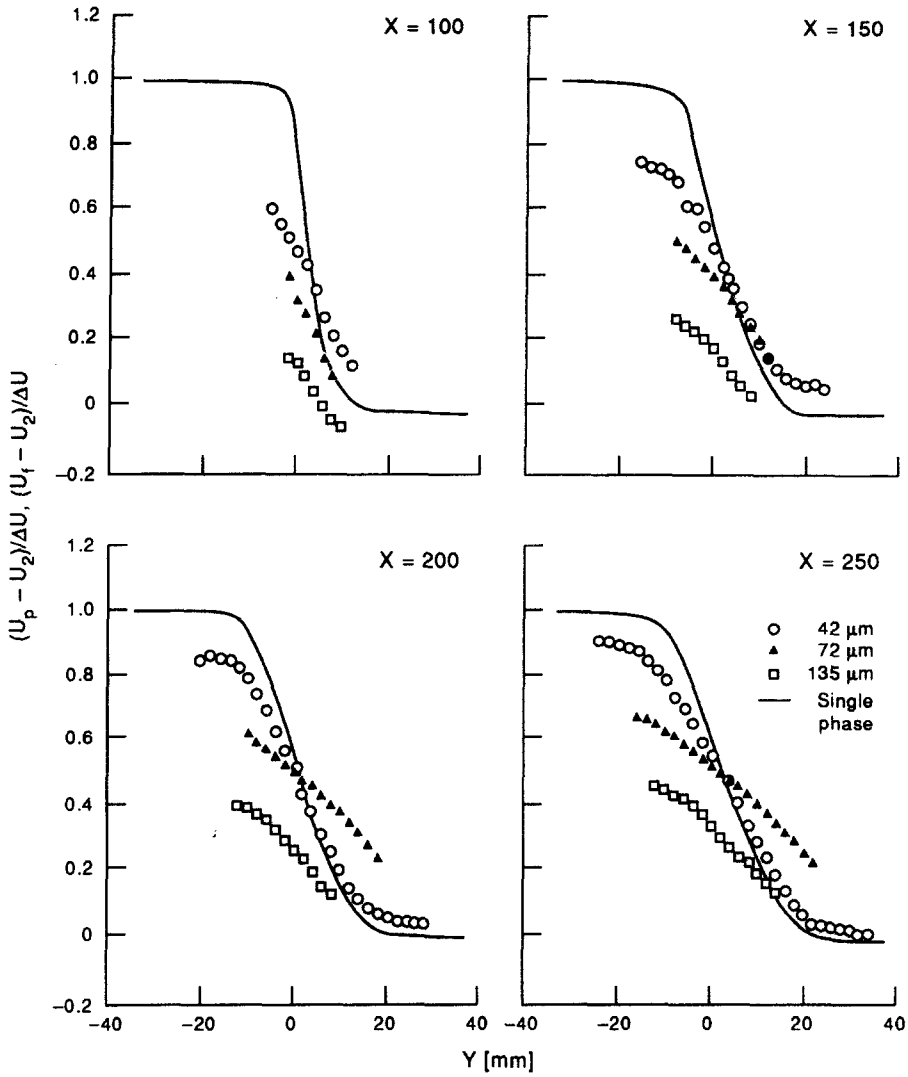

Figure 11. Distributions of particle mean velocity.

In general, particle velocity fluctuation approaches that of the gas phase with decreasing particle size and increasing width of the mixing layer. The lateral velocity fluctuation is much smaller than that in the streamwise direction. This feature is similar to the result of previous works by the authors for free (Fleckhaus *et al.* 1987) and confined jets (Hishida *et al.* 1989a, b). This phenomenon could be explained by considering the lateral motion of a particle which travels within a certain length scale such as the Lagrangian integral scale Λ_L. The particle, which moves toward the low-speed side by the vortex motion in the shear layer, cannot instantaneously follow the turbulent motion of the surrounding flow because the particle has inertia and does not have enough interaction time to follow the turbulent fluid motion. The differences in particle velocity between two points separated by the lateral distance Λ_L is approx. $\Lambda_L \cdot \partial U_p/\partial y$ for the streamwise component and $\Lambda_L \cdot \partial V_p/\partial y$ for the lateral component. In the present flow field particle velocities in the lateral direction are nearly zero and the velocity gradients of particles in the streamwise direction are much larger than those in the lateral direction. Consequently, the RMS value of the streamwise velocities of particles become larger than that of the lateral direction for the flow condition where a large velocity gradient exists in the streamwise direction.

Recently, Hardalupas *et al.* (1989) reported measurements in a two-phase free jet and explained the difference in the velocity fluctuations of particles in the axial and lateral directions. They called this phenomenon "fan spreading", i.e. the fact that $u'_p \gg v'_p$ is due to

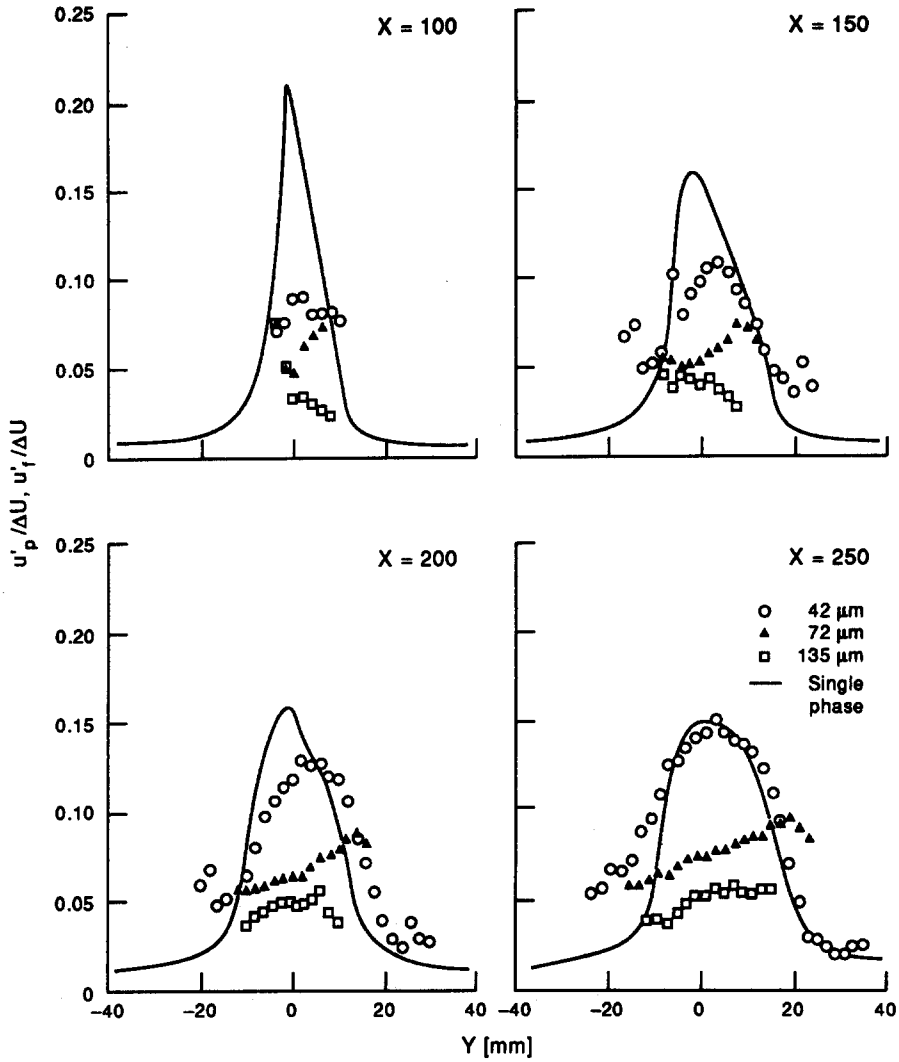

Figure 12. Distributions of velocity fluctuations of the gas and particle phases in the streamwise direction.

quasi-unidirectional trajectories of solid particles from the exit of the jet down to a certain streamwise distance.

However, even for flows where particles are unaffected by the initial condition, as indicated by the present results for mean velocity and the number density of particles, a similar behavior of $u'_p \gg v'_p$ exists. Particles in the developing shear layer have quasi-unidirectional trajectories caused by the interaction between the particles and the turbulence and/or vortex structure. This feature might also be explained by extending the "fan-spreading" effect.

The distributions of the $\overline{u_p v'_p}$-correlation are compared to the Reynolds shear stress of the gas phase in figure 14. The behavior of the $\overline{u'_p v'_p}$-correlation is the same as that of the velocity fluctuation discussed earlier. However, in the case of 42 and 72 μm particles, the values of the $\overline{u'_p v'_p}$-correlation near the outer edge of mixing layer, especially the low-speed side, become larger than those of single phase. This feature is considered to be due to the "overshoot" phenomenon of particle dispersion, i.e. a large-scale eddy pushes particles in the lateral direction within an interaction time which is of the same order of magnitude as the particle relaxation time. After reaching the outer edge of the mixing layer, the particle still keeps its motion due to its inertia. In the present flow, the particles are unable to follow the small-scale turbulent motion. Therefore, the effective scale of the turbulence eddies is considered to be a structural scale existing in the mixing layer.

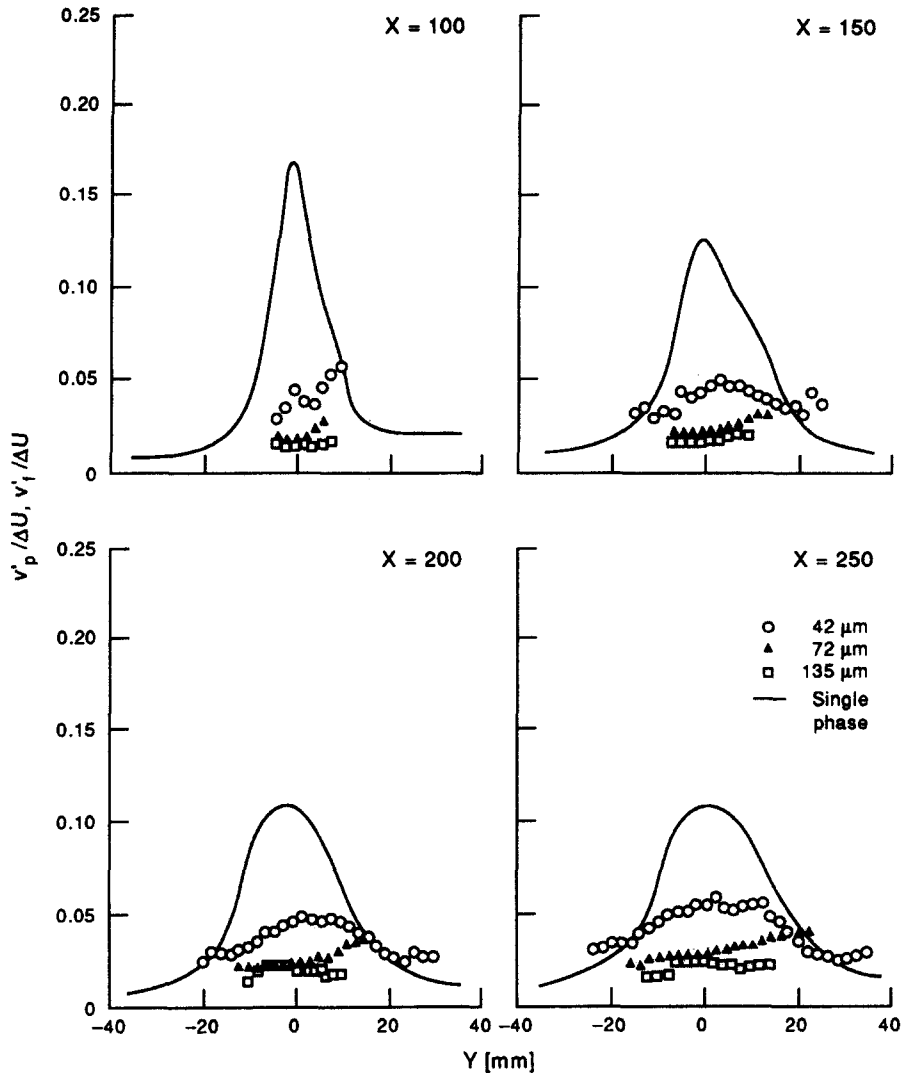

Figure 13. Distributions of velocity fluctuations of the gas and particle phases in the cross-stream direction.

For the 135 μm particles, almost uniform profiles of $\overline{u'v'}$ are found for all the experimental conditions. This confirms that these particles are hardly affected by the turbulent motion.

3.2.5. Particle dispersion in the mixing layer

In this section, an eddy diffusivity of particle ϵ_p is evaluated for discussion of the ability of a particle to follow the eddy motion.

The turbulent eddy diffusivity was introduced by Taylor through extending the concept of molecular diffusion for isotropic turbulent flow. It was confirmed after Taylor's study that the theory may be applied to non-isotropic turbulence in the mixing layer when dispersed particles exist in the turbulent gas flow (Snyder & Lumley 1971).

According to Taylor's diffusion theory, the mean square displacement $\overline{y^2(t)}$ of a fluid is given by

$$\overline{y^2(t)} = 2V_{L,P}^2 \int_0^t \int_0^{t'} R_L(\tau)\, d\tau\, dt', \qquad [5]$$

where $V_{L,P}$ is the Lagrangian velocity and $R_L(\tau)$ is the Lagrangian auto-correlation coefficient. When the diffusion time t is much smaller than the micro time scale τ_L, $R_L(\tau)$ becomes unity. Thus, [5] can then be written as

$$\overline{y^2(t)} = 2V_{L,P}^2 \cdot t^2. \qquad [6]$$

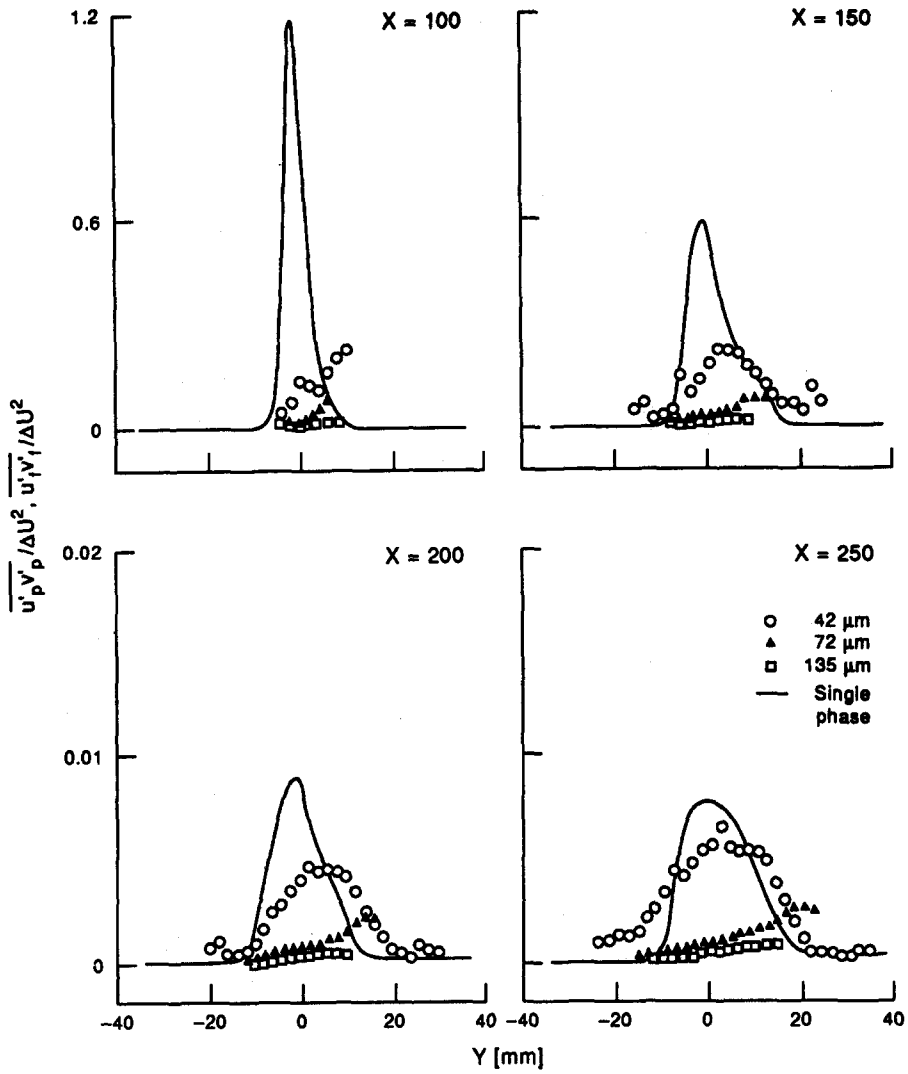

Figure 14. Distributions of the $\overline{u'v'}$-correlation.

The particle eddy diffusivity is defined as

$$\epsilon_p = \frac{1}{2}\frac{d}{dt}\overline{y^2(t)}. \quad [7]$$

Figure 15 shows the mean square displacement of particles in the Y direction, obtained from the measured results of particle number density, and t is diffusion time of the particle starting from the origin of flow mixing.

The diffusion time of the particles, t, is evaluated from the mean velocity U_{pm} averaged over all the particles in each cross section, as follows:

$$t = \int U_{pm}^{-1}\, dx, \quad [8]$$

where

$$U_{pm} = \frac{\sum_i (N_{d,i} \cdot U_{p,i})}{\sum_i N_{d,i}}. \quad [9]$$

U_{pm} is estimated by interpolation between the experimental data. In figure 15, the solid line expresses the following equation:

$$\overline{y^2(t)} = C \cdot t^2 \quad (C = \text{constant}). \qquad [10]$$

Equation [10] is similar to [6]. The mean displacement of the 135 μm particles is proportional to the square of t, which agrees with the equation of particle dispersion for a short diffusion time. Therefore, 135 μm particles are unaffected by turbulence, which is consistent with the results obtained from the particle velocity measurements shown in figures 11–14. The mean displacements of 42 and 72 μm particles deviate from [10] with increasing particle dispersion time and rapidly increase at $t = 0.02$ and 0.03 s, respectively.

Figure 16 indicates the relation between the ratio of particle eddy diffusivity, ϵ_p, to gas-phase eddy diffusivity, ϵ_f, in terms of St. Here, ϵ_f is evaluated from the width of the mixing layer δ, based on the Prandtl mixing model:

$$\epsilon_f = l_m^2 \left| \frac{\partial u}{\partial y} \right|, \qquad [11]$$

with

$$\frac{l_m}{\delta} = 0.07.$$

In view of the previous discussions on particle velocity characteristics, figure 16 describes three different stages of particle dispersion phenomena. For $0.5 < St < 2.5$, particles overshoot from the mixing layer and disperse faster than the fluid phase. In the range of $2.5 < St < 4$, particles disperse less with increasing St. Particles cannot follow the vortex motion of the mixing layer in the range of $St > 4$ and therefore disperse as in a homogeneous turbulent flow. This characteristic feature of the eddy diffusivity ratio having a maximum value at around $St = 1$ confirms the significance of time scales of large-scale eddies in determining particle motions and the overshoot phenomenon in particle dispersion, as indicated in the numerical calculation by Chein & Chung (1987) and Tang *et al.* (1989).

4. CONCLUDING REMARKS

An experimental study has been performed on particle dispersion in a mixing layer to clarify the significant factors which govern particle motion in turbulent flow. Spherical glass particles of 42, 72 and 135 μm arithmetic mean diameter were loaded into a two-dimensional air mixing layer. LDA enabled measurement of the two-component velocities of both the particles and the gas phase. The particle number density was also measured. The conclusions drawn from this work are as follows.

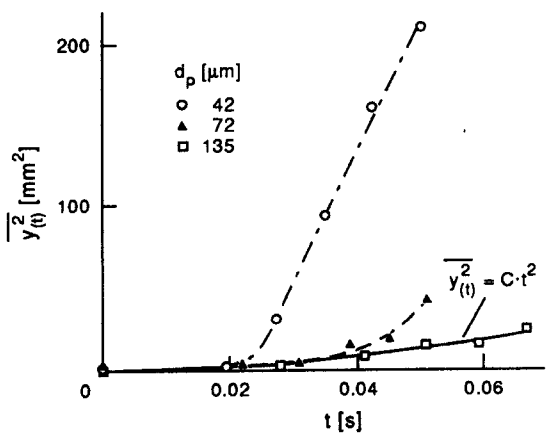

Figure 15. Variations of the lateral mean square displacement.

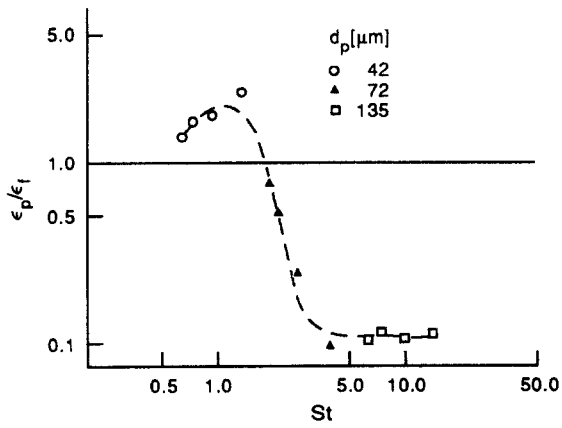

Figure 16. Variations of the particle eddy diffusivity with St.

The dispersion rate for the smaller particles, obtained from the particle number density measurements, was found to be larger than that of the fluid. That is, the particles can disperse further than the fluid phase. In contrast, larger particles are found to disperse as in isotropic turbulence, since these particles can hardly follow the fluid motion because of their larger inertia.

The characteristic behaviors in particle dispersion are well-correlated by St; the ratio of the particle relaxation time to the characteristics time scale of the large-scale eddies in the mixing layer. Therefore, particle dispersion strongly depends on the ability of particles to follow the motion of large-scale eddies in the turbulent flow. The range of St covered by the present study includes three different stages of particle dispersion phenomena: for the range of $St > 4$, the particles move independently of the turbulent motion of the continuous phase and its vortex motion hardly affects the particle dispersion; for the range of $2.5 < St < 4$, the particle eddy diffusivity rapidly increases with decreasing St; for the range of $0.5 < St < 2.5$, the particle dispersion coefficient becomes larger than the eddy diffusivity of the gas phase, i.e. particles disperse more significantly than the fluid phase.

Thus, the dominant factors governing the particle motion in a plane mixing layer have been quantified experimentally.

Acknowledgements—The authors would like to thank Messrs H. Sadata, Y. Ishima and N. Ohsawa for performing the experiments.

REFERENCES

BERLEMONT, A., DESJONQUERES, P. & GOUESBET, G. 1990 Particle Lagrangian simulation in turbulent flows. *Int. J. Multiphase Flow* **16,** 19–34.

BOOTHROYD, R. G. 1971 *Flowing Gas–Solids Suspensions.* Chapman & Hall, London.

BROWN, G. L. & ROSHKO, A. 1974 On density effects and large structure in turbulent mixing layers. *J. Fluid Mech.* **64,** 775–816.

CALABRESE, R. V. & MIDDLEMAN, S. 1979 The dispersion of discrete particles in a turbulent fluid field. *AIChE Jl* **25,** 1025–1035.

CHEIN, R. & CHUNG, J. N. 1987 Effects of vortex pairing on particle dispersion in turbulent shear flows. *Int. J. Multiphase Flow* **13,** 785–802.

CHEIN, R. & CHUNG, J. N. 1988 Simulation of particle dispersion in a two-dimensional mixing layer. *AIChE Jl* **34,** 946–954.

CHEN, C. P. & WOOD, P. E. 1986 Turbulence closure modelling of the dilute gas–particle axisymmetric jet. *AIChE Jl* **32,** 163–166.

DANON, H., WOLFSHTEIN, M. & HETSRONI, G. 1977 Numerical calculations of a two-phase turbulent round jet. *Int. J. Multiphase Flow* **3,** 223–234.

DIMOTAKIS, P. E. & BROWN, G. L. 1976 The mixing layer at high Reynolds number: large-structure dynamics and entrainment. *J. Fluid Mech.* **78,** 535–560.

ELGOBASHI, S., ABOU-ARAB, T., RIZK, M. & MOSTAFA, A. 1984 Prediction of the particle-laden jet with a two-equation turbulence model. *Int. J. Multiphase Flow* **10,** 697–710.

FLECKHAUS, D., HISHIDA, K. & MAEDA, M. 1987 Effect of laden solid particles on the turbulent flow structure of a round free jet. *Expts Fluids* **5,** 323–333.

HARDALUPAS, Y., TAYLOR, A. M. K. P. & WHITELAW, J. H. 1989 Velocity and particle-flux characteristics of turbulent particle-laden jets. *Proc. R. Soc. Lond.* **A426,** 31–78.

HISHIDA, K., MAEDA, M., IMARU, J., HIRONAGA, K. & KANO, H. 1984 Measurements of size and velocity of particle in two-phase flow by a three beam LDA system. In *Proc. Laser Anemometry in Fluid Mechanics*, LADOAN—Instituto Superior Tecnico, Lisbon, Portugal, pp. 121–136.

HISHIDA, K., UMEMURA, K. & MAEDA, M. 1986 Heat transfer to a plane wall jet in gas–solids two-phase flow. In *Proc. 8th Int. Heat Transfer Conf.*, San Francisco, CA, Vol. 5, pp. 2385–2390.

HISHIDA, K., TAKEMOTO, K. & MAEDA, M. 1987 Turbulence characteristics of a gas–solids two-phase confined jet (in Japanese). *Jap. J. Multiphase Flow* **1,** 56–69.

HISHIDA, K. NAKANO, H. & MAEDA, M. 1989a Turbulent flow characteristics of a liquid–solid particle confined jet. In *Proc. Int. Conf. on the Mechanics of Two-phase Flows*, Taipei, Taiwan, pp. 209–214.

HISHIDA, K., NAKANO, H., FUJISHIRO, T. & MAEDA, M. 1989b Turbulence characteristics of a liquid–solids two-phase circular confined jet (in Japanese). *Trans. JSME* **511,** 648–654.

HO, C.-M. & HUNG, L.-S. 1982 Subharmonics and vortex merging in mixing layers. *J. Fluid Mech.* **119,** 443–473.

HUSSAIN, A. K. M. F. & ZAMAN, K. B. M. Q. 1985 An experimental study of organized motions in the turbulent plane mixing layer. *J. Fluid Mech.* **159,** 85–104.

LEE, S. L. & DURST, F. 1982 On the motion of particles in turbulent duct flows. *Int. J. Multiphase Flow* **8,** 125–146.

LEE, K. B. & CHUNG, M. K. 1987 Refinement of the mixing-length model for prediction of gas–particle flow in a pipe. *Int. J. Multiphase Flow* **13,** 275–282.

MAEDA, M., KIYOTA, H. & HISHIDA, K. 1982 Heat transfer to gas–solid two-phase flow in separated, reattached and redevelopment regions. In *Proc. 7th Int. Heat Transfer Conf.*, Munich, Germany, Vol. 5, pp. 249–254.

MELVILLE, W. K. & BRAY, K. N. C. 1979 A model of the two-phase turbulent jet. *Int. J. Heat Mass Transfer* **22,** 647–656.

MIKSAD, R. W. 1972 Experiments on the nonlinear stages of the free–shear-layer transition. *J. Fluid Mech.* **56,** 695–719.

MILOJEVIC, D. & DURST, F. 1989 Lagrangian modeling of gas–particle jet flows and comparison with existing experimental data. In *Proc. Int. Conf. on the Mechanics of Two-phase Flows*, Taipei, Taiwan, pp. 145–151.

MODARESS, D., TAN, H. & ELGOBASHI, S. 1984 Two-component LDA measurement in a two-phase turbulent jet. *AIAA Jl* **22,** 624–630.

OSTER, D. & WYGNANSKI, I. 1982 The forced mixing layer between parallel streams. *J. Fluid Mech.* **123,** 91–130.

PARTHASARATHY, R. N. & FAETH, G. M. 1987 Structure of particle-laden turbulent water jets in still water. *Int. J. Multiphase Flow* **13,** 699–716.

PICART, A., BERLEMONT, A. & GOUESBET, G. 1986 Modelling and predicting turbulence fields and the dispersion of discrete particles transported by turbulent flows. *Int. J. Multiphase Flow* **12,** 237–261.

SHUEN, J.-S., SOLOMON, A. S. P., ZHANG, Q.-F. & FAETH, G. M. 1985 Structure of particle-laden jets: measurements and prediction. *AIAA Jl* **23,** 396–404.

SNYDER, W. H. & LUMLEY, J. L. 1971 Some measurements of particle velocity autocorrelation functions in a turbulent flow. *J. Fluid Mech.* **48,** 41–71.

SUN, T-Y., PARTHASARATHY, R. N. & FAETH, G. M. 1986 Structure of bubbly round condensing jets. *Trans. ASME Jl Heat Transfer* **108,** 951–959.

TANG, L., CROWE, C. T., CHUNG, J. N. & TROUTT, T. R. 1989 Effect of momentum coupling on the development of the shear layers in gas–particle mixtures. In *Proc. Int. Conf. on the Mechanics of Two-phase Flows*, Taipei, Taiwan, pp. 387–391.

WELLS, M. R. & STOCK, D. E. 1983 The effects of crossing trajectories on the dispersion of particles in a turbulent flow. *J. Fluid Mech.* **136,** 31–62.

WINANT, C. D. & BROWAND, F. K. 1974 Vortex pairing: the mechanism of turbulent mixing-layer growth at moderate Reynolds number. *J. Fluid Mech.* **63,** 237–255.